Intermittency of acceleration in isotropic turbulence

Sang Lee and Changhoon Lee*
Department of Mechanical Engineering, Yonsei University, 134 Shinchon-dong, Seodaemun-gu Seoul, 120-749, Korea
(Received 21 January 2005; published 31 May 2005)

The intermittency of acceleration is investigated for isotropic turbulence using direct numerical simulation. Intermittently found acceleration of large magnitude always points towards the rotational axis of a vortex filament, indicating that the intermittency of acceleration is associated with the rotational motion of the vortices that causes centripetal acceleration, which is consistent with the reported result for the near-wall turbulence. Furthermore, investigation on movements of such vortex filaments provides some insights into the dynamics of local dissipation, enstrophy and acceleration. Strong dissipation partially covering the edge of a vortex filament shows weak correlation with enstrophy, while it is strongly correlated with acceleration.

DOI: 10.1103/PhysRevE.71.056310 PACS number(s): 47.27.Gs, 02.70.Hm, 02.50.Fz

I. INTRODUCTION

Acceleration in fluid flow that causes erratic fluctuating motions of fluid particles is an important element in modelling turbulence. It is fundamental to transport, mixing and dispersion in the atmospheric transport as well as mixing processes in stirred chemical reactors and dispersion of nanoparticles. Such importance has led to many investigations on fluid particle acceleration in turbulence. For example, recent experimental studies [1,2] have shown that the fluid acceleration occurs in a very intermittent fashion. Moreover, the normalized acceleration variance is found to be dependent upon the Reynolds number up to $R_\lambda \sim 970$ [1]. Here, R_λ denotes the Taylor-scale Reynolds number. A numerical study by Vedula *et al.* [3] shows that such R_λ dependence can be observed at R_λ as low as 40, suggesting that these characteristics of accelerations are related to coherent structures of fluid motions. Mordant *et al.* [4] has claimed that the long time correlation of acceleration magnitude is the key to the intermittent behavior. From a recent study of accelerations in the near-wall turbulence [5], it has been shown that the pressure gradient in the near-wall coherent vortical structures, which is the dominant contributor to acceleration, points towards the center of the axis of the coherent vortical structure. This suggests that the centripetal force due to the rotational motion of the coherent vortical structures, which have values exceeding 20 times its root-mean-square (rms) value, is the dominant source of acceleration intermittency. Still, the question of whether it is the case in general remains unanswered. Recently, Biferale *et al.* [6] showed that the multifractal formalism can predict the wide nature of probability density function (PDF) of acceleration, without providing a dynamical content.

In this study, we have carried out direct numerical simulation of isotropic turbulence in a three-dimensional periodic domain with $R_\lambda = 44$ and 66 to investigate the intermittent behavior of acceleration and its dominant source. Furthermore, we investigate how local dissipation is related to acceleration and local enstrophy raised by Zeff *et al.* [7].

II. KINEMATICS OF ACCELERATIONS

In order to obtain the statistics of acceleration, the Navier-Stokes equations with continuity are solved by using direct numerical simulation (DNS). The dimension of the computational domain is $2\pi \times 2\pi \times 2\pi$, and a spectral method is used to expand the flow variables on 128^3 numerical grids. For the temporal integration of the nonlinear terms and forcing, the second-order Adams-Bashforth method is adopted while the viscous terms are computed using the Crank-Nicolson method. A skew-symmetric form [8] is used for the nonlinear terms, which is energy-conserving and minimizes the aliasing errors. To maintain the equilibrium state, the lowest wavenumber components of the velocity are artificially forced, hardly affecting the small scales. A more detailed description of the numerical method used can be found in Lee and Seo [9]. The terms on the right-hand side of the Navier-Stokes equation can be decomposed into a sum of contributions from the pressure gradient ($\mathbf{a}^I$), which is irrotational (or potential), and the viscous force ($\mathbf{a}^S$), which is solenoidal for constant density flow.

$$\frac{\partial \mathbf{u}}{\partial t} + (\mathbf{u} \cdot \nabla)\mathbf{u} = -\frac{1}{\rho}\nabla p + \nu \nabla^2 \mathbf{u} = \mathbf{a}^I + \mathbf{a}^S. \qquad (1)$$

Here, p is the pressure, $\mathbf{u}$ the velocity, ρ the density, and ν the molecular viscosity. In the near-wall turbulent flow, the viscous force has a noticeable effect on acceleration in the region very close to the wall. For an isotropic case, however, the viscous force becomes very small and almost negligible as the Reynolds number increases [3,10,11]. Therefore, it is of our interest to focus on the statistics of the pressure gradient.

Figure 1 shows an example of a coherent vortical structure, the so-called vortex filament, represented by an image of iso-surface of enstrophy defined by $\Omega \equiv \boldsymbol{\omega} \cdot \boldsymbol{\omega}/2$ with $\boldsymbol{\omega}$ denoting vorticity vector. Local maximum enstrophy is found at the axis of rotation as can be observed in the cross section of the vortex filament. Instantaneous accelerations of magnitude 20 times rms value are always observed near a filament, pointing towards the rotation axis, which suggests that the centripetal force associated with the rotational motion of a vortex filament is the dominant source of intermit-

*Electronic address: clee@yonsei.ac.kr

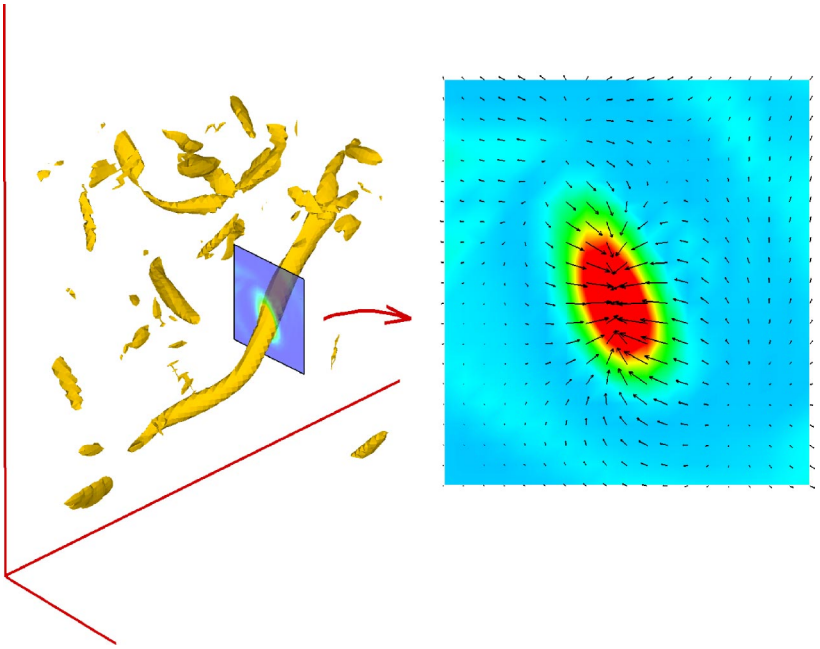

FIG. 1. (Color online) Isosurface of enstrophy at $R_\lambda = 44$ along with its cross section, in which pressure gradient is shown as arrows. Arrows with large magnitude inside the core of the vortex filament point toward the center of rotation, which are mostly parallel with the enstrophy's gradient.

tency. This is consistent with the previous study on the near-wall turbulence [5].

A qualitative inspection of angle between the negative pressure gradient and the enstrophy gradient has been performed. In Fig. 2, we plot the mean squared pressure gradient conditioned on the angle, defined by

$$\cos\beta = \frac{-\nabla p \cdot \nabla \Omega}{|\nabla p||\nabla \Omega|}. \tag{2}$$

As shown in Fig. 2, large pressure gradients mostly occur when the angle between the two vectors is almost zero, with the PDF of β (inset) diminishing to almost zero at $\beta = 0$, indicating that intermittently found large pressure gradients are mostly parallel with the enstrophy gradient. Thus, this figure serves as a quantitative evidence supporting that the intermittent acceleration is caused by the centripetal force (pressure gradient) associated with the rotational motion of vortex filaments in isotropic turbulence, similar to the result for the near-wall turbulence [5] and a recent study by Mordant *et al.* [12]. Compared to the near-wall turbulence [5], a strong correlation between the pressure gradient and enstrophy gradient is more pronounced in the present isotropic flow. From Fig. 2, the steepening of the curve near $\beta = 0$ is observed as R_λ increases, while the PDF of β for both Reynolds numbers are identical.

Figure 3 shows the PDF of normalized acceleration in one direction at $R_\lambda = 44$ and 66, featuring very long stretched exponential tails. The flatness factor of acceleration was computed to be 13.25 and 19.46 for $R_\lambda = 44$ and 66, respectively. The increasing probability of acceleration of large magnitude at higher R_λ is in good agreement with the previous studies [1,2]. The large accelerations shown in the ends of the tail are associated with vortex filaments, which persist for many eddy turnover times. a_0, defined by $a_0 = \langle a_i a_i \rangle / 3 \langle \epsilon \rangle^{3/2} \nu^{-1/2}$, with $\langle \epsilon \rangle$ mean dissipation, is a universal constant at high

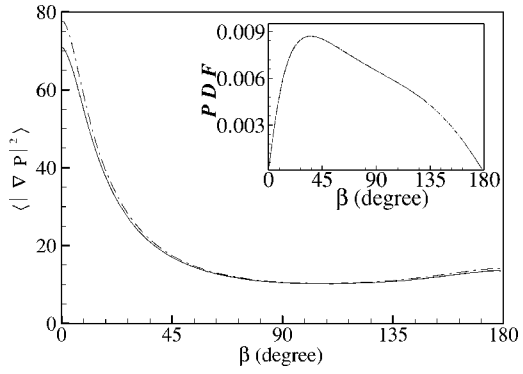

FIG. 2. Mean squared pressure gradient conditioned on angle between pressure gradient and enstrophy gradient for $R_\lambda = 44$ (solid line) and 66 (dash-dot line). Here, the mean squared pressure gradient is arbitrarily nondimensionalized. The magnitude of mean squared pressure gradient is at its maximum when the two vectors are parallel. The inset contains the PDF of the angle β.

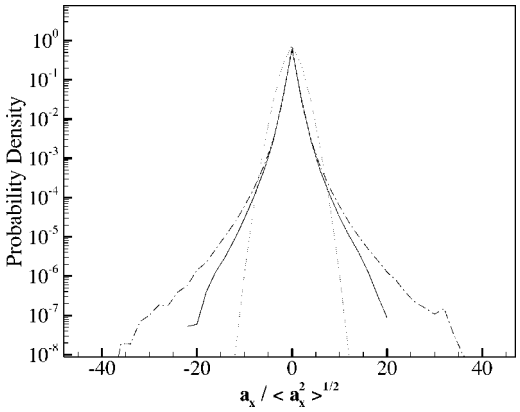

FIG. 3. Probability density function of acceleration normalized by rms value at $R_\lambda = 44$ (solid) and 66 (dash-dot) with Gaussian distribution (dots).

Reynolds number according to the Kolmogorov's hypothesis [13,14]. Here, the bracket denotes ensemble-averaged quantity. In our study, a_0 is 2.14 and 2.63 for $R_\lambda = 44$ and 66, respectively. The R_λ dependency is well known from the previous DNS results [3,15] as well as experimental observations [1,2,16,17], which is $a_0 \sim R_\lambda^{1/2}$ with R_λ up to 500. Unfortunately, the number of cases considered in the present study is too few to confirm the trend as suggested by previous authors. But the importance lies in the increasing trend, which is a good indication of increasing intermittency of acceleration with the Reynolds number.

If the coherent structures are the main sources of acceleration intermittency, it would be interesting to know the conditions on the formation of such structures. Studies by Cao, Chen, Doolen [18], and Pumir [19] suggested by visual inspection of isosurfaces of pressure that the vortex filaments begin to form at around $R_\lambda \sim 70$. The pressure PDF with R_λ larger than 70 begins to show superexponential tail, resulting in a leap of the pressure flatness at $R_\lambda \sim 70$, which was used as an indicator of existence of such vortex filaments. Our DNS results at $R_\lambda = 44$ (Fig. 1), however, show that such vortex filaments are observed from a three-dimensional view of enstrophy isosurfaces, indicating that $R_\lambda \sim 70$ may not be the physical transitional point. The λ_2 method [20] also shows the existence of such structures very clearly (figure not shown).

III. RELATIONS BETWEEN ACCELERATION, DISSIPATION AND ENSTROPHY

The local dissipation rate ϵ, which is known to have relevance to the intermittency of enstrophy [7], is investigated. The correlations between ϵ, the absolute value of acceleration $|\mathbf{a}|$ and Ω obtained from 4.2×10^7 data are shown in Fig. 4. It can be observed that large acceleration is accompanied by strong local dissipation, while the opposite does not necessarily hold true, as has been found from other studies [5,7].

A visual inspection of local dissipation shown in Fig. 5 reveals that local dissipation, which is a measure of irrotational strain, is not only strong in the edges of vortex filaments, but also in the area between the vortex filaments where acceleration is relatively low. This helps to explain why strong local dissipation is not always accompanied by large accelerations and enstrophy. However, a strong correlation between large acceleration and strong dissipation can be observed from Fig. 4(a), similar to the results by Mordant *et al.* [12], in which the joint probability between strong dissipation and large acceleration is high, while small values of acceleration and dissipation have a very low joint probability. Similarly, it is further shown that large enstrophy and strong dissipation have a high joint probability [7,12]. However, for $\Omega/\langle\Omega\rangle$ greater than 20, mostly found in vortex filaments, local dissipation is uncorrelated in comparison with the same acceleration scale in Fig. 4(a). Although the scatter width of the dissipation magnitude becomes narrow with increasing enstrophy, the width is still too wide even at $\Omega/\langle\Omega\rangle$ greater than 50. Since strong local dissipation lies mostly outside of the vortex filaments, while Ω has its local maximum at the center of the vortex filaments, the uncorrelated result is not surprising in Fig. 4(b).

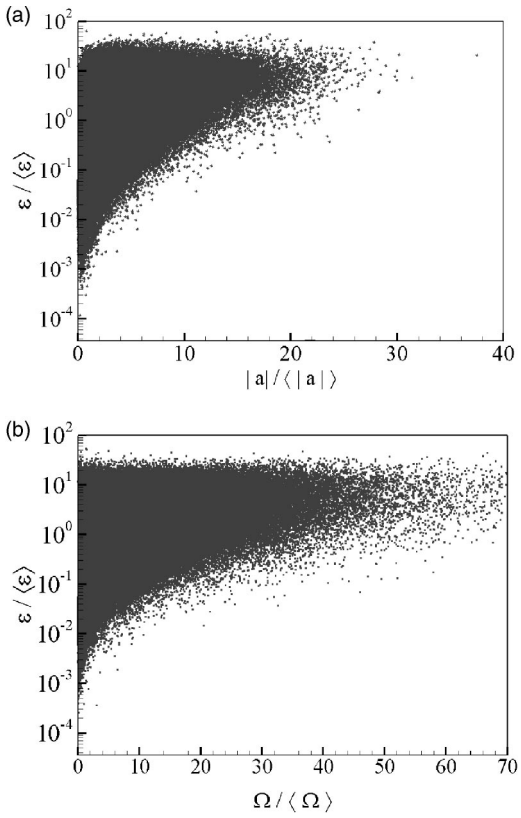

FIG. 4. Correlation plots for (a) $\epsilon - |\mathbf{a}|$ and (b) ϵ-Ω normalized by their own ensemble means. Large acceleration is accompanied by strong dissipation. However, strong dissipation is not always associated with acceleration of large magnitude. ϵ-Ω plot shows a similar trend. However, for $\Omega/\langle\Omega\rangle \sim 20$, ϵ and Ω is uncorrelated in comparison with the same acceleration scale in (a).

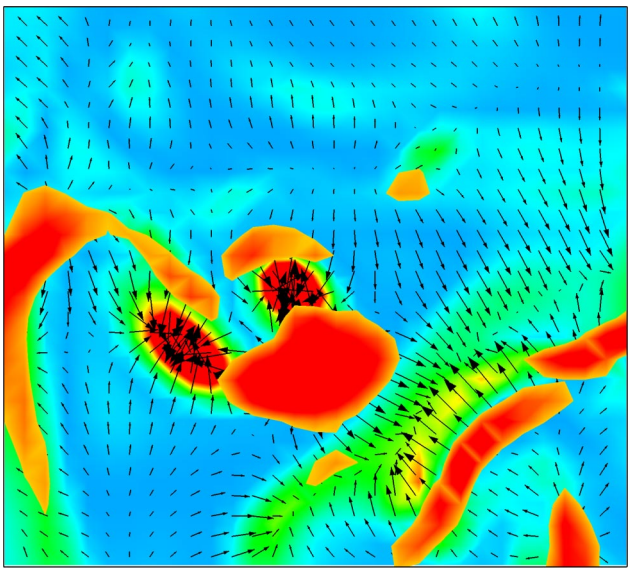

FIG. 5. (Color online) Contours of enstrophy with pressure gradient vectors. Dark (orange in color) regions without arrows in them are regions of strong local dissipation, lying on the edges of the vortex filaments and between vortical structures.

A little manipulation of Eq. (1) yields

$$\frac{1}{\rho}\nabla^2 p = \Omega - \frac{\epsilon}{2\nu}. \tag{3}$$

Taking gradient of Eq. (3) under the incompressibility condition leads to

$$\frac{1}{\rho}\nabla^2(\nabla p) = \nabla\Omega - \frac{\nabla\epsilon}{2\nu}, \tag{4}$$

clearly indicating that the source of ∇p, the main contributor to acceleration, comprises two vectors, gradients of enstrophy and dissipation. Given that both enstrophy and dissipation are highly intermittent, it is expected that intermittently large acceleration is found at the edges of strong peaks of either enstrophy or dissipation unless enstrophy and dissipation cancel out each other. As shown in Fig. 5, such a complete cancellation is not likely. Instead, in many cases, they are found close to each other, resulting in a very large pressure gradient between the peaks of enstrophy and dissipation, where gradient vectors of enstrophy and dissipation are opposite to each other. However, enstrophy is mostly found to be more intermittent and local than dissipation, thus the contribution from enstrophy is dominant as confirmed in the statistics of β shown in Fig. 2. The leading-order cancellation between enstrophy and dissipation claimed by Nelkin [21] does not seem to occur at least at this Reynolds number.

According to the previous experimental study by Zeff *et al.* [7], a typical sequence of intense strain and vorticity growth due to the intermittent nature of turbulence is the following: an intense local dissipation over 10 times its rms value grows rapidly and the enstrophy grows in the same order of value with some delay, and finally decays to its random fluctuating values. To investigate the dynamics of local dissipation and enstrophy in more detail, we have recorded data from 27 locations within the computational domain, similar to the experiments by Zeff *et al.* [7] in obtaining the local strain and enstrophy in a very small region of $1.8\eta^3$ scale. Here, η is the Kolmogorov length scale. Similar cases of intense peak of dissipation followed by enstrophy peak were observed. However, from investigation of many cases, we found that the order of sequence is random.

Two possible explanations suggested for this phenomenon were advection of vortex structures and local generation of intense dissipation and enstrophy [7]. As have been found in Fig. 5, intense dissipation lies mostly on the edges of vortex filaments having local maximum enstrophy at the rotational axis. This picture provides an interesting clue that the consecutive peaks of local dissipation and enstrophy may be due to advection of a vortex filament. That is, the probe will experience strong dissipation and subsequent large enstrophy as the regions of intense strain and vorticity pass through. By sampling the three-dimensional data at every $0.1376\tau_\eta$, the animation showed smooth movement of the vortex filaments (Fig. 6). Here, τ_η is the Kolmogorov time scale. Although a generalized conclusion cannot be drawn from an animation of the vortex and local strain structure, all 27 cases show advection of such structures rather than local generation and decay of intense strain and enstrophy. Figure 7 illustrates one

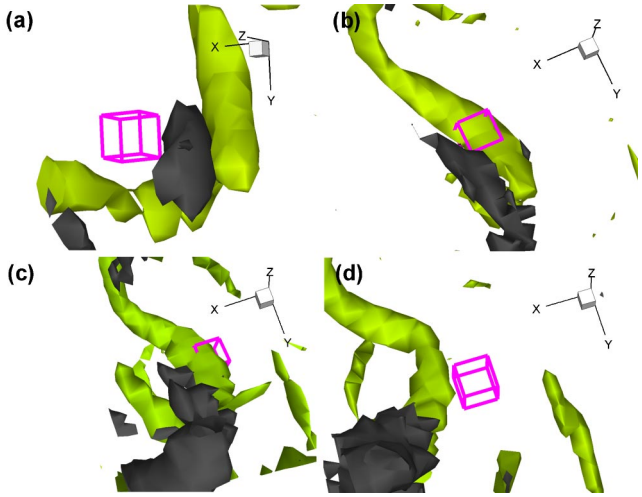

FIG. 6. (Color online) Movement of a vortex filament (light color) and local dissipation (dark color). The filament slowly passes through the center of the box, which records intense peaks of dissipation, enstrophy, and acceleration shown in Fig. 7.

example of rising local strain followed by growing enstrophy, similar to Zeff *et al.*'s result [7]. Since acceleration is large on the edges of the vortex filament, acceleration curve is also presented. Intense local strain region partially surrounding the vortex filament approaches the probing point as the value of local strain increases. As the filament migrates, the high vortical region enters as the strain decreases and enstrophy rapidly jumps to a high peak, and finally drops to the low random fluctuating values as the filament leaves the probing point. The magnitude of acceleration rises and falls at the entry and exit of the vortex filament. Sometimes the edge of the filament moves across the probe, showing almost coincidence of the two peaks. A close observation of Fig. 7 reveals that high peaks of dissipation and acceleration partially overlap with each other. Since strong dissipation lies in the edge of vortex filaments where acceleration (centripetal force) is also large, it is not surprising to see a strong corre-

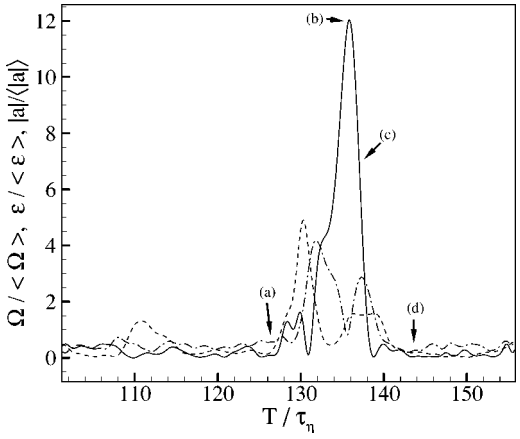

FIG. 7. Time histories of normalized dissipation (dots), acceleration (dash-dots) and enstrophy(solid). Four instances, marked by (a) through (d), correspond to times of each plate of Fig. 6, respectively. Note that time is nondimensionalized by the Kolmogorov time scale.

lation between large acceleration and intense dissipation as shown in Fig. 4(a).

IV. SUMMARY

From a direct numerical study of isotropic turbulence, it is found that large centripetal force associated with the rotational motion of the vortex filaments is found to be the dominant source of acceleration intermittency, which is consistent with the result for the near-wall turbulence [5]. This physical picture on acceleration intermittency could be very useful for understanding how nonextensive statistical mechanics [22,23] or multifractal formalism [6] can produce a wide PDF of acceleration, as well as for the development of the Lagrangian PDF model for acceleration [24,25]. Such vortex filaments are, in part, shown to be responsible for the reported correlation between intermittent dissipation and enstrophy [7]. Large acceleration and dissipation on the edge of the vortex filament shows a strong correlation, whereas enstrophy having its local maximum at the rotational axis shows a weak correlation with strong dissipation. It is observed that the sequence of high peaks of local dissipation, enstrophy and acceleration as measured at a fixed point is mostly due to the advection of a vortex filament, rather than local generation. Although the range of the Reynolds number considered in the present study is relatively low, such an intermittent nature of acceleration is expected to be more pronounced in high Reynolds number isotropic turbulence.

ACKNOWLEDGMENTS

We acknowledge support from the Korea Science and Engineering Foundation through Grant No. R01-2003-000-10124-0. A large portion of computation was carried out at KISTI Supercomputing Center.

[1] A. La Porta, G. A. Voth, A. M. Crawford, J. Alexander, and E. Bodenschatz, Nature (London) **409**, 1017 (2001).
[2] G. A Voth, A. La Porta, A. M Crawford, J. Alexander, and E. Bodenschatz, J. Fluid Mech. **469**, 212 (2002).
[3] P. Vedula and P. K. Yeung, Phys. Fluids **11**, 1208 (1999).
[4] N. Mordant, J. Delour, E. Leveque, A. Arneodo, and J. F. Pinton, Phys. Rev. Lett. **89**, 254502 (2002).
[5] C. Lee, K. Yeo, and J.-I. Choi, Phys. Rev. Lett. **92**, 144502 (2004).
[6] L. Biferale, G. Boffetta, A. Celani, B. J. Devenish, A. Lanotte, and F. Toschi, Phys. Rev. Lett. **93**, 064502 (2004).
[7] B. W. Zeff, D. D. Lanterman, R. McAllister, R. Roy, E. J. Kostelich, and D. P. Lathrop, Nature (London) **421**, 146 (2003).
[8] A. G. Kravchenko and P. Moin, J. Comput. Phys. **131**, 310 (1997).
[9] C. Lee and Y. Seo, J. Comput. Phys. **183**, 438 (2002).
[10] R. J. Hill and S. T. Thoroddsen, Phys. Rev. E **55**, 1600 (1997).
[11] M. Nelkin, Adv. Phys. **43**, 143 (1994).
[12] N. Mordant, E. Leveque, and J. Pinton, New J. Phys. **6**, 116 (2004).
[13] A. M. Yaglom, C. R. Acad. Sci. URSS **67**, 795 (1949).
[14] G. K. Batchelor, Proc. Cambridge Philos. Soc. **47**, 395 (1951).
[15] P. K. Yeung and S. B. Pope, J. Fluid Mech. **207**, 531 (1989).
[16] B. L. Sawford, P. K Yeung, M. S. Borgas, P. Vedula, A. La Porta, A. M. Crawford, and E. Bodenschatz, Phys. Fluids **15**, 3478 (2003).
[17] T. Gotoh and R. Rogallo, J. Fluid Mech. **396**, 257 (1999).
[18] N. Cao, S. Chen, and G. D. Doolen, Phys. Fluids **11**, 2235 (1999).
[19] A. Pumir, Phys. Fluids **6**, 2071 (1994).
[20] J. Jeong and A. Hussain, J. Fluid Mech. **285**, 69 (1994).
[21] M. Nelkin, Phys. Fluids **11**, 2202 (1999).
[22] C. Beck, Phys. Rev. Lett. **87**, 180601 (2001).
[23] C. Beck, Phys. Lett. A **287**, 240 (2001).
[24] A. M. Reynolds, Phys. Fluids **15**, L1 (2003).
[25] A. M. Reynolds, K. Yeo, and C. Lee, Phys. Rev. E **70**, 017302 (2004).